Organo-palladium(II) complexes bearing unsymmetrical *N,N,N*-pincer ligands: synthesis, structures and oxidatively induced coupling reactions†

Luka A. Wright,[a] Eric G. Hope,[a] Gregory A. Solan,*[a] Warren B. Cross[a,b] and Kuldip Singh[a]

The 2-(2′-aniline)-6-imine-pyridines, 2-(C₆H₄-2′-NH₂)-6-(CMe═NAr)C₅H₃N (Ar = 4-i-PrC₆H₄ (H**L1a**), 2,6-i-Pr₂C₆H₃ (H**L1b**)), have been synthesised *via* sequential Stille cross-coupling, deprotection and condensation steps from 6-tributylstannyl-2-(2-methyl-1,3-dioxolan-2-yl)pyridine and 2-bromonitrobenzene. The palladium(II) acetate *N,N,N*-pincer complexes, [{2-(C₆H₄-2′-NH)-6-(CMe═NAr)C₅H₃N}Pd-(OAc)] (Ar = 4-i-PrC₆H₄ (**1a**), 2,6-i-Pr₂C₆H₃ (**1b**)), can be prepared by reacting H**L1** with Pd(OAc)₂ or, in the case of **1a**, more conveniently by the template reaction of ketone 2-(C₆H₄-2′-NH₂)-6-(CMe═O)-C₅H₃N, Pd(OAc)₂ and 4-isopropylaniline; ready conversion of **1** to their chloride analogues, [{2-(C₆H₄-2′-NH)-6-(CMe═NAr)C₅H₃N}PdCl] (Ar = 4-i-PrC₆H₄ (**2a**), 2,6-i-Pr₂C₆H₃ (**2b**)), has been demonstrated. The phenyl-containing complexes, [{2-(C₆H₄-2′-NH)-6-(CMe═NAr)C₅H₃N}PdPh] (Ar = 4-i-PrC₆H₄ (**3a**), 2,6-i-Pr₂C₆H₃ (**3b**)), can be obtained by treating H**L1** with (PPh₃)₂PdPh(Br) in the presence of NaH or with regard to **3a**, by the salt elimination reaction of **2a** with phenyllithium. Reaction of **2a** with silver tetrafluoroborate or triflate in the presence of acetonitrile allows access to cationic [{2-(C₆H₄-2′-NH)-6-(CMe═N(4-i-PrC₆H₄)C₅H₃N}Pd(NCMe)][X] (X = BF₄ (**4**), X = O₃SCF₃ (**5**)), respectively; the pyridine analogue of **5**, [{2-(C₆H₄-2′-NH)-6-(CMe═N(4-i-PrC₆H₄)C₅H₃N}Pd(NC₅H₅)][O₃SCF₃], is also reported. Oxidation of phenyl-containing **3a** with one equivalent of 1-chloromethyl-4-fluoro-1,4-diazoniabicyclo-[2.2.2]octane bis(tetrafluoroborate) (Selectfluor™) in acetonitrile at low temperature leads to a new palladium species that slowly decomposes to give **4** and biphenyl; biphenyl formation is also observed upon reaction of **3a** with XeF₂. However, no such oxidatively induced coupling occurs when using **3b**. Single crystal X-ray diffraction studies have been performed on H**L1b**, **1a**, **1b**, **2a**, **2b**, **3a**, **3b** and **5′**.

Introduction

Recent years have seen a surge of interest in oxidatively induced coupling reactions involving Pd(III) and Pd(IV) intermediates due, in part, to their potential to promote transformations inaccessible using the conventional low valent Pd(0)/(II) cycle.[1–3] For example, the historically challenging arene–fluoride bond forming reaction has become a reality with both types of high valent intermediate isolated and/or proposed in reaction pathways derived from Pd(II) species.[3] Central to these

developments have been reagents such as Selectfluor™ [1-chloromethyl-4-fluoro-1,4-diazoniabicyclo[2.2.2]octane bis-(tetrafluoroborate)] and xenon difluoride that can oxidise the metal centre as a two electron oxidant (from Pd(II) to Pd(IV))[4,5] or as a one electron oxidant (from Pd(II) to Pd(III))[6,7] and moreover provide a source of F (*e.g.*, as F⁺ or F˙). In cases where these types of oxidant deliver a fluorine atom direct to the metal centre, selective C–F reductive elimination from the high valent organo–metal intermediate can be challenging as alternative (and potentially desirable) degradation pathways can prove competitive.[3d] Sanford, for example, has reported that the Pd(IV) mono-aryl complex, [(4,4-*t*-Bu₂bipy)Pd(Ar)-(F)₂(FHF)] (Ar = 4-FC₆H₄), only undergoes selective C_aryl–F reductive elimination when heated in the presence of excess oxidant, otherwise competitive Ar–Ar coupling occurs through a process described as σ-aryl exchange between metal centres.[5] Indeed this type of intermolecular Ar–Ar coupling involving palladium mono-aryl species has some precedent in Pd(II) and

[a]Department of Chemistry, University of Leicester, University Road, Leicester LE1 7RH, UK. E-mail: gas8@leicester.ac.uk

[b]School of Science and Technology, Nottingham Trent University, Clifton Lane, Nottingham NG11 8NS, UK
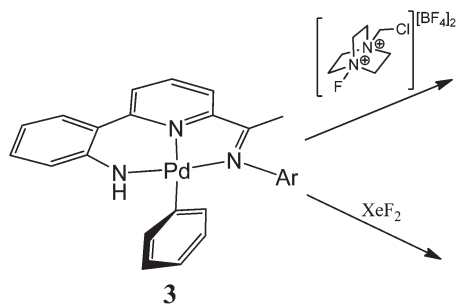
Fig. 1 *N,N,N* palladium(II) mono-aryl pincer, **3**, and the stoichiometric reactivity to be examined.

Pd(III) chemistry involving complexes bearing a variety of multidentate ligands.[2c,8,9]

Given the apparent variation in coupling events that can occur from a high valent organo-Pd species,[1–7] we have been interested in exploring the influence of a supporting multidentate ligand on the oxidatively induced reaction pathway. Herein, we report the reactivity of a family of *N,N,N*-pincer bearing Pd(II) mono-phenyl complexes of the type, [{2-(C_6H_4-2-NH)-6-(CMe=NAr)C_5H_3N}PdPh] (Ar = aryl (**3**)), towards Selectfluor and XeF_2 (Fig. 1);[10] as an additional point of interest the effects that steric variation (Ar = 4-i-PrC_6H_4, 2,6-i-$Pr_2C_6H_3$) has on the reactivity, will be investigated. Furthermore, we report the full synthetic details for the preparation of the novel pro-ligands (**HL1**) and their palladium(II) acetate (**1**), chloride (**2**) and phenyl (**3**) derivatives.

Results and discussion

Preparation of pro-ligand HL1

The 2-(2′-aniline)-6-imine-pyridines, 2-(C_6H_4-2′-NH_2)-6-(CMe=NAr)C_5H_3N (Ar = 4-i-PrC_6H_4 (**HL1a**), 2,6-i-$Pr_2C_6H_3$ (**HL1b**)), have been prepared in reasonable yield *via* sequential Stille coupling, deprotection and condensation reactions from 6-tributylstannyl-2-(2-methyl-1,3-dioxolan-2-yl)pyridine and 2-bromonitrobenzene (Scheme 1). For both **HL1a** and **HL1b**, the condensation step proved sluggish in alcoholic media but proceeded more effectively by running the reaction in the neat aniline at high temperature; nevertheless problems encountered in the work-up of **HL1a** resulted in its isolation in only a
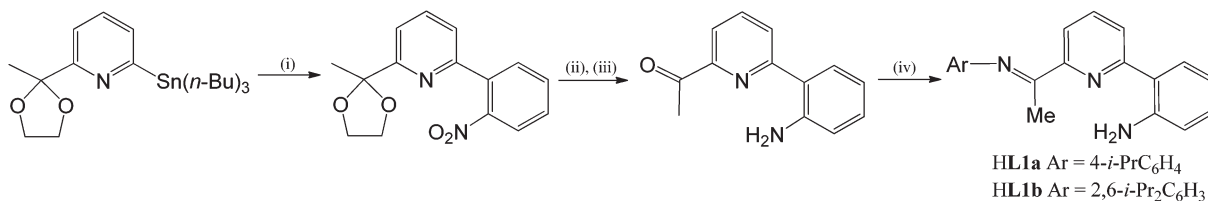
modest yield (see later for a higher yielding template approach to **L1a**). The precursor ketone and the two *N,N,N* pro-ligands, **HL1a** and **HL1b**, have been characterised using a combination of electrospray mass spectrometry, IR, ^{1}H NMR and ^{13}C NMR spectroscopy (see Experimental section).

Compounds, **HL1a**, and **HL1b**, both display protonated molecular ions peaks in their electrospray mass spectra and downfield shifted signals for the amino protons (range: δ 5.72–5.79) in their ^{1}H NMR spectra. Characteristic imine stretching frequencies of *ca.* 1638 cm^{-1} are seen in their IR spectra as are higher wavenumber bands corresponding to the N–H stretches. Further confirmation of the composition of **HL1b** was achieved in the form of a single crystal X-ray determination.

A perspective view of **HL1b** is depicted in Fig. 2; selected bond distances and angles are listed in Table 1. The structure consists of a central pyridine ring that is substituted at its 2-position by a phenyl-2′-amine group and at the 6-position by a *trans*-configured *N*-arylimine unit [C(7)–N(1) 1.277(3) Å]. The pyridine nitrogen atoms adopt a *cis* conformation with respect to the neighbouring aniline nitrogen (tors: N(2)–C(13)–C(14)–C(15) 8.1°) as a result of a hydrogen-bonding interaction between one of the amino hydrogen atoms and the pyridine nitrogen [N(3)···N(2) 2.675 Å]; a similar arrangement has been reported for a related quinolinyl-substituted aniline.[11]

Palladium(II) complexes of L1

Interaction of **HL1b** with Pd(OAc)$_2$ at 60 °C in toluene gave on work-up, [{2-(C_6H_4-2-NH)-6-(CMe=N(2,6-i-$Pr_2C_6H_3$))C_5H_3N}Pd(OAc)] (**1b**)), in good yield (Scheme 2). While [{2-(C_6H_4-2-NH)-6-(CMe=N(4-i-PrC_6H_4))C_5H_3N}Pd(OAc)] (**1a**) could also be made by this route, it was more conveniently prepared by the template reaction of ketone 2-(C_6H_4-2-NH_2)-6-(CMe=O)C_5H_3N, Pd(OAc)$_2$ and 4-isopropylaniline. Compounds **1** can be readily converted to their chloride analogues, [{2-(C_6H_4-2-NH)-6-(CMe=NAr)C_5H_3N}PdCl] (Ar = 4-i-PrC_6H_4 (**2a**), 2,6-i-$Pr_2C_6H_3$ (**2b**)), by treatment of a dichloromethane solution of **1** with aqueous sodium chloride. All four complexes are air stable and have been characterised using a combination of FAB mass spectrometry, IR and NMR (^{1}H and ^{13}C) spectroscopy and elemental analyses (see Experimental section). In addition, crystals of each complex have been the subject of single crystal X-ray diffraction studies.

Scheme 1 *Reagents and conditions*: (i) 2-$BrC_6H_4NO_2$, cat. Pd(OAc)$_2$–PPh$_3$, toluene, 100 °C, microwave; (ii) $SnCl_2$, ethanol; (iii) HCl(aq.); (iv) $ArNH_2$, 225 °C.
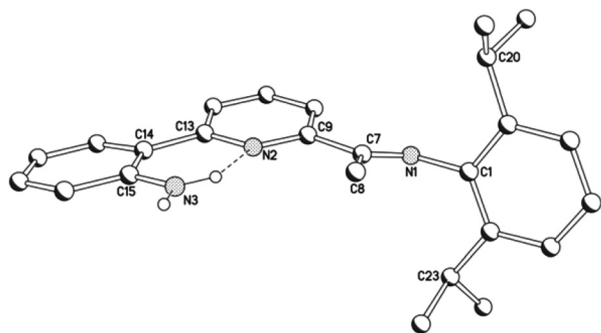
Fig. 2 Molecular structure of **HL1b**, including a partial atom numbering scheme. All hydrogen atoms, apart from H3A and H3B, have been omitted for clarity.

Table 1 Selected bond distances (Å) and angles (°) for **HL1b**

Bond lengths			
C(15)–N(3)	1.366(4)	C(13)–C(14)	1.477(4)
C(7)–N(1)	1.277(3)	C(7)–C(9)	1.482(4)
C(7)–C(8)	1.504(4)		
Bond angles			
C(8)–C(7)–N(1)	125.3(2)	C(9)–C(7)–N(1)	116.4(3)

Views of acetate-containing **1a** and **1b** are given in Fig. 3 and 4; selected bond distances and angles are collected for both structures in Table 2. There are two independent molecules for **1b** in the unit cell (*A* and *B*) which differ most noticeably in the relative inclination of neighbouring pyridyl and anilido ring planes (*vide infra*). The structures of **1a** and **1b** are similar consisting of a four-coordinate palladium centre bound by a tridentate monoanionic 2-(2′-anilido)-6-imine-pyridine ligand and a monodentate *O*-bound acetate, but contrast in the nature of the hydrogen bonding involving the acetate ligand. In **1a**, a water molecule present within the unit cell links the palladium-acetate units to form a hydrogen-bonded network [O(1)$_{acetate}$···O(3)$_{water}$ 2.837, O(3)$_{water}$···O(2A)$_{acetate}$ 2.877 Å], while in **1b** the hydrogen bonding is intramolecular in origin involving the pendant acetate oxygen and the anilido proton [N(3)···O(2)$_{acetate}$ 2.799$_A$, 2.889$_B$ Å]. Within the *N,N,N*-ligand there are both 5- and 6-membered chelate rings with the bite angle for the 6-membered ring being more compatible with the square planar geometrical requirements of the
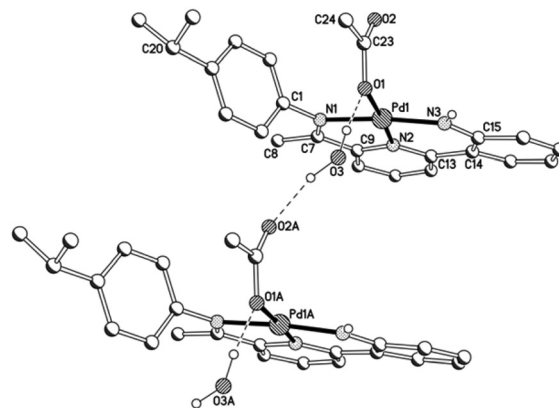

Fig. 3 A segment of the network based on **1a** linked by water molecules. A partial atom numbering scheme is included while all hydrogen atoms, apart from H3 and those belonging to the water molecule, have been omitted for clarity; dotted lines show the intermolecular hydrogen-bonding interactions.
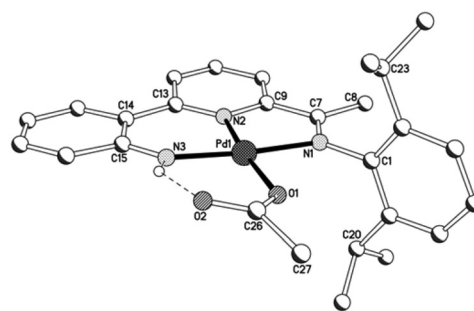

Fig. 4 Molecular structure of **1b** (molecule A) including a partial atom numbering scheme. All hydrogen atoms, apart from H3 have been omitted for clarity.

palladium(II) centre [N(3)–Pd(1)–N(2)$_{6-membered}$: 93.7(2) (**1a**), 92.2(3)$_A$, 93.6(2)$_B$ (**1b**) *vs.* N(2)–Pd(1)–N(1)$_{5-membered}$ 82.2(2) (**1a**), 82.6(3)$_A$, 82.1(2)$_B$° (**1b**)]. In both cases some twisting of the anilido unit with respect to the adjacent pyridyl plane is apparent [tors. N(2)–C(13)–C(14)–C(15) 3.6(4) (**1a**), 4.9(4)$_A$, 9.0(5)$_B$° (**1b**)]. For a given complex, the Pd–N$_{imine}$ bond distance is the longest of the three metal–ligand interactions involving the *N,N,N*-ligand followed by the Pd–N$_{pyridine}$ distance and then by the Pd–N$_{anilido}$ distance which is best exemplified for **1a**

Scheme 2 *Reagents and conditions*: (i) Pd(OAc)$_2$, toluene, 60 °C; (ii) NaCl(aq.), CH$_2$Cl$_2$, RT.

Table 2 Selected bond distances (Å) and angles (°) for **1a** and **1b**

		1b	
	1a	Molecule A	Molecule B
Bond lengths			
Pd(1)–N(1)	2.014(6)	2.017(8)	2.019(8)
Pd(1)–N(2)	1.963(5)	1.970(9)	1.977(7)
Pd(1)–N(3)	1.932(5)	1.920(9)	1.922(8)
Pd(1)–O(1)	2.036(5)	2.011(8)	2.021(7)
C(7)–N(1)	1.286(8)	1.285(12)	1.300(11)
C(9)–C(7)	1.469(9)	1.468(13)	1.458(13)
C(15)–N(3)	1.347(9)	1.316(12)	1.323(12)
Bond angles			
N(1)–Pd(1)–N(2)	82.2(2)	82.6(3)	82.1(2)
N(1)–Pd(1)–N(3)	174.6(3)	174.3(3)	174.4(2)
N(1)–Pd(1)–O(1)	93.8(2)	89.6(3)	93.8(2)
N(2)–Pd(1)–N(3)	93.7(2)	92.2(3)	93.6(2)
N(3)–Pd(1)–O(1)	90.3(2)	95.6(3)	90.5(2)

Table 3 Selected bond distances (Å) and angles (°) for **2a** and **2b**

	2a		2b
	Molecule A	Molecule B	
Bond lengths			
Pd(1)–N(1)	2.022(5)	2.035(6)	2.025(3)
Pd(1)–N(2)	1.976(5)	1.984(5)	1.987(3)
Pd(1)–N(3)	1.934(5)	1.931(6)	1.927(3)
Pd(1)–Cl(1)	2.2971(18)	2.2931(18)	2.3123(17)
C(7)–N(1)	1.297(7)	1.298(7)	1.289(5)
C(15)–N(3)	1.335(8)	1.334(8)	1.336(5)
Bond angles			
N(1)–Pd(1)–N(2)	81.6(2)	82.2(3)	82.01(13)
N(1)–Pd(1)–N(3)	174.4(2)	174.0(2)	173.63(13)
N(2)–Pd(1)–N(3)	93.1(2)	92.2(3)	91.91(13)
N(1)–Pd(1)–Cl(1)	96.66(16)	96.56(17)	97.63(10)
N(2)–Pd(1)–Cl(1)	178.21(17)	175.39(15)	179.27(9)
N(3)–Pd(1)–Cl(1)	88.54(16)	89.14(17)	88.47(10)

$[Pd(1)–N(1)_{imine}$ 2.014(6) > $Pd(1)–N(2)_{pyridine}$ 1.963(5) > $Pd(1)–N(3)_{anilido}$ 1.932(5) Å]. The *N*-aryl groups are inclined towards orthogonality with regard to the neighbouring $C{=}N_{imine}$ vector [tors. C(7)–N(1)–C(1)–C(6) 87.6(4) (**1a**), 86.4(4)$_{av}°$ (**1b**)], with the 2,6-diisopropyl substitution on the *N*-aryl group in **1b** additionally providing some steric protection to the axial sites of the palladium centre. The closest crystallographically characterised comparators to **1** are the phenolate-containing counterparts, $[\{2-(C_6H_4-2'-O)-6-(CMe{=}NAr)C_5H_3N\}Pd(OAc)]$ (Ar = 4-i-PrC$_6$H$_4$, 2,6-i-Pr$_2$C$_6$H$_3$), which display similar bonding characteristics.[12]

A view of chloride-containing **2b** is given in Fig. 5; selected bond distances and angles are collected for both **2a** and **2b** in Table 3. The two independent molecules present in the unit cell for **2a** (A and B) differ most noticeably in the inclination of the *N*-aryl plane to the adjacent imine unit. The structures of **2a** and **2b** are similar to those of their acetate precursors (**1**) with a tridentate monoanionic 2-(2'-anilido)-6-imine-pyridine filling three coordination sites of the distorted square planar geometry but differ with a chloride now filling the fourth site.

Replacing a chloride for an *O*-bound acetate has little effect on the *trans* Pd–N$_{pyridine}$ distance [1.976(5)$_A$, 1.984(5)$_B$ (**2a**), 1.987(3) (**2b**) *vs.* 1.963(5) (**1a**), 1.970(9)$_A$ 1.977(7)$_B$ Å (**1b**)]. Unlike **1b**, the anilido NH proton is not involved in any inter- or intra-molecular contacts of note.

Complexes **1a**, **1b**, **2a** and **2b**, all display molecular ion peaks in their FAB mass spectra along with fragmentation peaks corresponding to the loss of an acetate or a chloride, respectively. In their IR spectra the imine stretching frequencies are shifted between 28 and 35 cm^{-1} to lower wavenumber in comparison with the corresponding free H**L1**, characteristic of imine-nitrogen coordination.[13–15] In **1b** and **2b** two distinct doublets are seen for the isopropyl methyl groups in their ^{1}H NMR spectra consistent with some restricted rotation about the *N*-2,6-diisopropylphenyl bond in solution. The acetate methyl groups in **1** can be seen at δ *ca.* 1.5 in their ^{1}H NMR spectra with the Me*C*(O)O carbon atoms observable at δ *ca.* 177.1 in their ^{13}C NMR spectra. The anilido NH proton in **2** is observable at a similar chemical shift (*ca.* δ 5.8) to that seen in free H**L1**, but in acetate-containing **1** there is some variation with that observed in **1b** being more downfield (δ 5.60 (**1a**), 7.39 (**1b**)); this is likely to be due to the influence of the intra-molecular NH⋯O$_{acetate}$ hydrogen bonding seen in **1b** (see Fig. 4). As with related monodentate acetate complexes, **1a** and **1b** both show strong bands assignable to the symmetric and asymmetric ν(COO) vibrations.[16]

Their phenyl derivatives, $[\{2-(C_6H_4-2-NH)-6-(CMe{=}NAr)-C_5H_3N\}PdPh]$ (Ar = 4-i-PrC$_6$H$_4$ (**3a**), 2,6-i-Pr$_2$C$_6$H$_3$ (**3b**)), could be readily accessed by treatment of H**L1** with NaH followed by (PPh$_3$)$_2$PdPh(Br) (Scheme 3). Alternatively, **3a** can be prepared by treating chloride **2a** with phenyl lithium; a related salt elimination approach to make **3b** has not proved possible. In the case of **2a**, chloride abstraction with both silver tetrafluoroborate and triflate in acetonitrile proved facile affording $[\{2-(C_6H_4-2'-NH)-6-(CMe{=}N(4-i-PrC_6H_4)C_5H_3N\}Pd(NCMe)][X]$ (X = BF$_4$ (**4**), X = O$_3$SCF$_3$ (**5**)) in high yield (Scheme 3). Mono-phenyl **3a** and **3b** are air and water stable, whereas **4** and **5** proved hygroscopic on prolonged standing. All four complexes

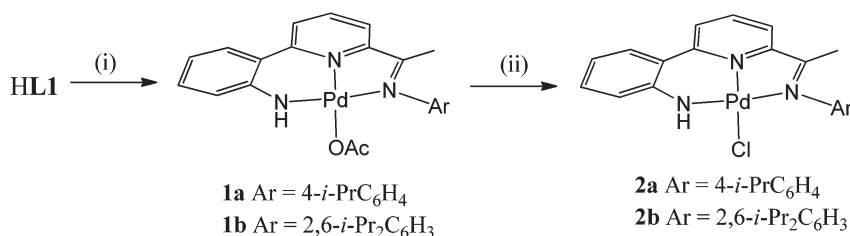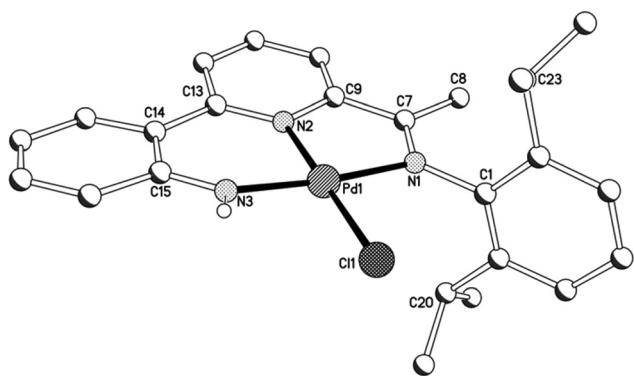**Fig. 5** Molecular structure of **2b** including a partial atom numbering scheme. All hydrogen atoms, apart from H3, have been omitted for clarity.

Scheme 3 Reagents and conditions: (i) xs. NaH, THF, heat; (ii) (PPh₃)₂PdPh(Br), THF, heat; (iii) LiPh, THF, −78 °C; (iv) AgX (X = BF₄, O₃SCF₃), MeCN, RT.

have been characterised using a combination of FAB mass spectrometry, IR and NMR (^{1}H and ^{13}C) spectroscopy and elemental analyses (see Experimental section).

The mass spectra of **3a** and **3b** exhibit molecular ions while **4** and **5** display peaks corresponding to their cationic units. As with **1** and **2**, all four complexes exhibit ν(C=N)$_{imine}$ stretches at lower wavenumber (typically by 35 cm^{-1}) when compared with **HL1**, supporting coordination of **L1** to the metal centre.[13–15] The imine methyl resonances are seen between δ 2.2 and 2.5 in their ^{1}H NMR spectra, while signals for the imine carbon fall between δ 170.5 and 174.8 in their ^{13}C{^{1}H} NMR spectra. Signals attributable to [BF₄]⁻ and [O₃SCF₃]⁻ counterions could also be seen in the ^{19}F NMR spectra of **4** and **5**. In addition, crystals of **3a**, **3b** and the pyridine analogue of **5**, [{2-(C₆H₄-2′-NH)-6-(CMe=N(4-i-PrC₆H₄)C₅H₃N}Pd(NC₅-H₅)][O₃SCF₃] (**5′**), have been the subject of single crystal X-ray diffraction studies.

As a representative of the mono-phenyl pair of structures, a view of the molecular structure of **3a** is depicted in Fig. 6; selected bond distances and angles are listed in Table 4 for both **3a** and **3b**. As with **1** and **2**, 2-(2′-anilido)-6-imine-pyridine ligand acts a tridentate ligand with the σ-phenyl ligand now occupying the fourth coordination site to complete a distorted square planar geometry. The phenyl ligand in both structures is tilted with respect to the trans-pyridine unit of the N,N,N-ligand and most noticeably for **3a**, presumably as a consequence of the variation in steric hindrance imposed by the N-aryl groups [tors. C(13)–N(2)–C(23)–C(24) 46.4(4) (**3a**),

Fig. 6 Molecular structure of **3a** including a partial atom numbering scheme. All hydrogen atoms, apart from H3, have been omitted for clarity.

Table 4 Selected bond distances (Å) and angles (°) for **3a** and **3b**

	3a	3b
Bond lengths		
Pd(1)–N(1)	2.060(6)	2.041(2)
Pd(1)–N(2)	2.066(6)	2.069(2)
Pd(1)–N(3)	1.937(6)	1.959(3)
Pd(1)–C(23)	2.016(8)	2.013(3)
C(7)–N(1)	1.302(9)	1.291(4)
C(9)–C(7)	1.452(10)	1.472(4)
C(15)–N(3)	1.326(9)	1.348(4)
Bond angles		
N(1)–Pd(1)–N(2)	81.0(3)	79.88(10)
N(1)–Pd(1)–N(3)	172.5(3)	171.38(10)
N(1)–Pd(1)–C(23)	99.2(3)	99.68(11)
N(2)–Pd(1)–C(23)	178.5(3)	169.73(11)
N(3)–Pd(1)–N(2)	91.5(3)	79.88(10)

41.4(4)° (**3b**)]. When compared to **1** and **2**, the presence of a σ-phenyl group in **3** results in an elongation of the trans Pd–N$_{pyridine}$ distance [Pd–N(2) 2.066(6) (**3a**), 2.069(2) (**3b**) vs. 1.963(5) (**1a**), 1.974(8)$_{av.}$ (**1b**), 1.980(5)$_{av.}$ (**2a**), 1.987(3) (**2b**) Å], an observation attributable to the strong trans-influence exhibited by the aryl group. In contrast, the exterior nitrogen-palladium distances remain similar in length to those seen in **1** and **2**. To accommodate the increased Pd–N(2)$_{pyridine}$ distance, there is increased twisting of the ligand backbone which is most apparent in **3b** [tors. N(2)–C(13)–C(14)–C(15) 25.2(4) and N(1)–C(7)–C(9)–N(2) 13.7(4)°]. As with chloride-containing **2**, the anilido NH proton shows no notable intra- or inter-molecular contacts of note.

Unfortunately cationic **4** and **5** were not amenable to forming crystals suitable for an X-ray determination. To overcome this practical issue, small amounts of pyridine were added to a solution of **5** in chloroform and hexane slowly diffused forming single crystals of [{2-(C₆H₄-2′-NH)-6-(CMe= N(4-i-PrC₆H₄)C₅H₃N}Pd(NC₅H₅)][O₃SCF₃] (**5′**). The molecular structure of the cationic unit **5′** is depicted in Fig. 7; selected bond distances and angles are listed in Table 5. As with a number of the structures reported in this study, two independent molecules (A and B) were present in the unit cell which, in this case, differ most noticeably in the inclination of the N-aryl groups. The structure of **5′** consists of a palladium(II) cationic unit charge balanced by a non-coordinating triflate counteranion. Within the distorted square planar cationic
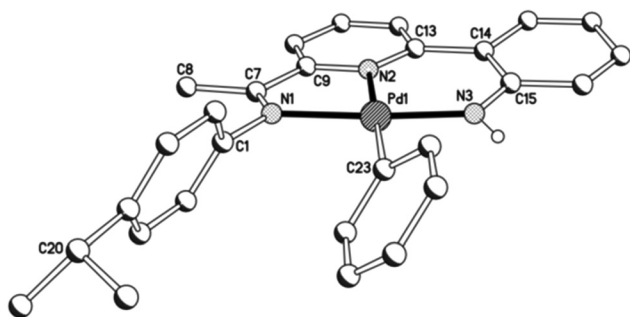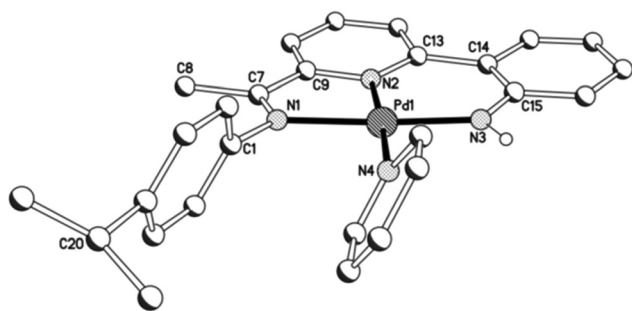
Fig. 7 Molecular structure of cationic unit in **5′**, including a partial atom numbering scheme. All hydrogen atoms, except for H3, have been omitted for clarity.

Table 5 Selected bond distances (Å) and angles (°) for **5′**

	Molecule A	Molecule B
Bond lengths		
Pd(1)–N(1)	2.049(12)	2.034(12)
Pd(1)–N(2)	1.992(11)	1.952(11)
Pd(1)–N(3)	1.937(11)	1.962(11)
Pd(1)–N(4)	2.010(11)	2.105(11)
C(7)–N(1)	1.276(16)	1.279(16)
C(15)–N(3)	1.336(15)	1.316(16)
Range S–O (triflate)	1.424(11)–1.485(10)	
Bond angles		
N(1)–Pd(1)–N(2)	82.9(5)	82.0(5)
N(1)–Pd(1)–N(3)	175.3(5)	174.9(4)
N(1)–Pd(1)–N(4)	93.7(5)	94.0(5)
N(2)–Pd(1)–N(3)	92.6(5)	93.8(5)
N(2)–Pd(1)–N(4)	176.6(5)	175.7(5)
N(3)–Pd(1)–N(4)	90.8(5)	90.3(4)

unit, the 2-(2′-anilido)-6-imine-pyridine ligand acts a tridentate ligand and an *N*-bound pyridine fills the fourth coordination site. Similar to phenyl-bound **3**, the monodentate hetero-aromatic in **5′** is not co-planar with the *trans*-pyridine unit of the tridentate ligand. Instead it adopts a tilted configuration [C(13)–N(2)–N(4)–C(27) 58.1(5)$_A$, 60.0(5)$_B$°] which is *ca.* 8° greater than that for the aryl group in **3b**. Inspection of the *trans* Pd–N(2)$_{pyridine}$ distance involving the *N*,*N*,*N*-ligand reveals a bond length [Pd(1)–N(2) 1.992(11)$_A$, 1.952(11)$_B$ Å] comparable with those seen in **1** and **2**, but shorter than that in **3** (*vide supra*). The NH proton of the anilido unit of the
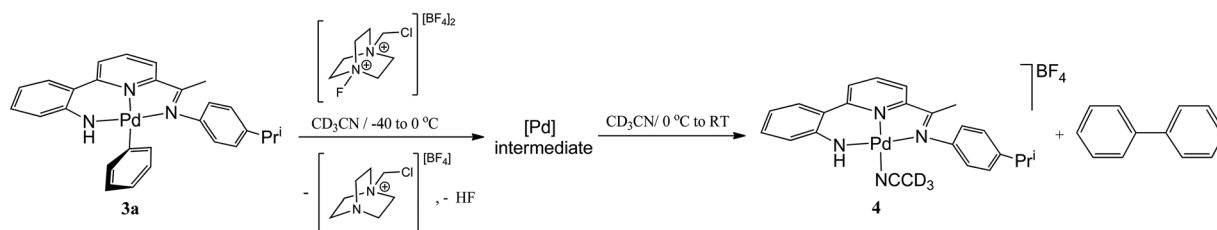
pincer undergoes a modest interaction with a triflate oxygen atom [N(3)···O(1) 3.096$_A$, 3.175$_B$ Å].

Reactivity of 3 towards Selectfluor and XeF$_2$

In the first instance the reactivity of mono-phenyl containing **3a** towards Selectfluor was explored. Typically **3a** was treated with excess Selectfluor at 100 °C in a toluene–MeCN mixture; these higher temperature conditions having been identified as more conducive to formation of the C–F reductive elimination product.[4c,3c] However, biphenyl was the only aryl-containing organic product identified by GC-MS. Likewise using XeF$_2$ as the oxidant instead of Selectfluor under the same conditions gave only biphenyl.

To investigate the reaction further and potentially observe any possible intermediates, a reaction involving an equimolar ratio of **3a** and Selectfluor was undertaken in CD$_3$CN at a series of lower temperatures and the reaction monitored by ^{1}H and ^{19}F NMR spectroscopy (Scheme 4). After 15 minutes at room temperature the ^{19}F NMR spectrum revealed full consumption of Selectfluor and a new peak at δ −181 attributable to the formation of hydrogen fluoride.[17] The ^{1}H NMR spectrum contained signals consistent with biphenyl, the salt [{2-(C$_6$H$_4$-2-NH)-6-(CMe═N(4-i-PrC$_6$H$_4$)C$_5$H$_3$N}Pd(NCCD$_3$)][BF$_4$] (**4**) (*vide supra*) and 1-(chloromethyl)-1,4-diazabicyclo[2.2.2]-octan-1-ium tetrafluoroborate, the Selectfluor degradation product. In addition, there were signals present attributable to another palladium species that slowly reduced in intensity over time.

When the reaction was carried out at −40 °C, full consumption of Selectfluor was again evident from the ^{19}F NMR spectrum which also contained a peak attributable to HF, albeit temperature shifted (δ −172). In the ^{1}H NMR spectrum full conversion of **3a** to a single palladium species was observed with the aromatic/pyridyl region integrating to sixteen protons; no peaks assignable to biphenyl nor **4** could be identified. As the reaction mixture was warmed to 0 °C, only sharpening of the ^{1}H NMR spectrum was observed with peaks that clearly match those observed for the decomposing palladium species seen at room temperature (Fig. S9 in ESI†). In the ^{19}F NMR spectrum a 1 : 8 ratio between the HF signal (δ −174) and the BF$_4$ peak (δ −152) accounts for all the fluorine introduced from the Selectfluor (Fig. S10 in ESI†). On warming to room temperature, decomposition of the palladium intermediate ensued generating biphenyl and **4**; full conversion being

Scheme 4 Low temperature oxidation of **3a** and Ar−Ar coupling on warming.

observed after 48 hours (Fig. S11 in ESI†). Unfortunately, further attempts to fully characterise the high valent palladium intermediate were unsuccessful.

The 1 : 1 reaction of 2,6-diisopropylphenyl-containing **3b** with Selectfluor was also explored at a range of different temperatures. However, despite consumption of **3b**, there was no evidence for the formation of biphenyl, fluorobenzene nor could any characterisable palladium species be identified. It is unclear as to the origin of these differences in reactivity between **3a** and **3b** towards Selectfluor.

Conclusions

A new family of imino-based monoanionic N,N,N pincer ligands have been developed that can support neutral palladium(II) acetate (**1**), chloride (**2**) and phenyl (**3**) species; the tetrafluoroborate (**4**) and triflate (**5**) salts are also reported. The oxidatively induced Ph–Ph coupling reactions involving **3a** described in this work highlights the ability of Selectfluor and xenon difluoride to behave as bystanding oxidants.[3d] Using the more sterically bulky **3b**, neither biphenyl nor fluorobenzene were produced under similar oxidative conditions. The identity of the palladium intermediate that generates biphenyl and cationic **4** remains uncertain but investigations into the precise nature of this species are ongoing.

Experimental

General

All operations, unless otherwise stated, were carried out under an inert atmosphere of dry, oxygen-free nitrogen using standard Schlenk and cannular techniques or in a nitrogen purged glove box. Operations involving a Microwave were performed on a CEM Discover Explorer Hybrid instrument. Solvents were distilled under nitrogen from appropriate drying agents[18] or were employed directly from a Solvent Purification System (Innovative Technology, Inc.). The electrospray (ESI) mass spectra were recorded using a micromass Quattra LC mass spectrometer with acetonitrile or methanol as the matrix. FAB mass spectra (including high resolution) were recorded on a Kratos Concept spectrometer with NBA as matrix or on a Waters Xevo QToF mass spectrometer equipped with an atmospheric solids analysis probe (ASAP). The infrared spectra were recorded in the solid state with Universal ATR sampling accessories on a Perkin Elmer Spectrum One FTIR instrument. NMR spectra were recorded on a Bruker DRX400 spectrometer at 400.13 (^{1}H), 376.46 (^{19}F) and 100.61 MHz (^{13}C) or a Bruker Avance III 500 spectrometer at 125 MHz (^{13}C), at ambient temperature unless otherwise stated; chemical shifts (ppm) are referred to the residual protic solvent peaks and coupling constants are expressed in hertz (Hz). Melting points (mp) were measured on a Gallenkamp melting point apparatus (model MFB-595) in open capillary tubes and were uncorrected. Elemental analyses were performed at the Science

Technical Support Unit, London Metropolitan University. The reagents 4-isopropylaniline, 2,6-diisopropylaniline, tin(II) chloride dihydrate, phenyllithium (1.8 M in n-Bu$_2$O), silver triflate, silver tetrafluoroborate, 1-chloromethyl-4-fluoro-1,4-diazoniabicyclo[2.2.2]octane bis(tetrafluoroborate) (Selectfluor™) and 2-bromonitrobenzene were purchased from Aldrich Chemical Co. and used without further purification. The compounds 6-tributylstannyl-2-(2-methyl-1,3-dioxolan-2-yl)pyridine[19] and [(PPh$_3$)$_2$PdPh(Br)][20] were prepared using literature procedures. All other chemicals were obtained commercially and used without further purification.

Synthesis of 2-(2-methyl-1,3-dioxolan-2-yl)-6-(2-nitrophenyl)-pyridine

A 25 mL microwave vial was loaded with 2-bromonitrobenzene (0.536 g, 2.70 mmol), 6-tributylstannyl-2-(2-methyl-1,3-dioxolan-2-yl)pyridine (1.226 g, 2.70 mmol), Pd(OAc)$_2$ (0.025 g, 0.11 mmol) and triphenylphosphine (0.058 g, 0.22 mmol) and the contents dissolved in bench toluene (13 mL). The system was then sealed and stirred for 30 s in a microwave before heating to 100 °C (with 100 W power and 10 bar pressure limits) for 1 h. The resulting dark brown reaction mixture was concentrated under reduced pressure to yield a dark brown oil. This oil was then dry loaded on to a silica column and eluted with a 70 : 30 mixture of petroleum ether (40–60) and ethyl acetate affording 2-(2-methyl-1,3-dioxolan-2-yl)-6-(2-nitrophenyl)-pyridine as a yellow solid (0.517 g, 67%) along with trace amounts of the homocoupled by-product 6,6′-bis(2-methyl-1,3-dioxolan-2-yl)-2,2′-bipyridine. ^{1}H NMR (400 MHz, CDCl$_3$): δ 1.66 (s, 3H, CH$_3$), 3.84 (m, 2H, O–CHH–CHH–O), 4.02 (m, 2H, O–CHH–CHH–O), 2.37 (dd, $^3J_{HH}$ 7.8, $^4J_{HH}$ 1.0, 1H, Ar–H), 7.42–7.46 (m, 1H, Ar–H), 7.50 (dd, $^3J_{HH}$ 7.5, $^4J_{HH}$ 0.9, 1H, Ar–H), 7.54–7.57 (m, 2H, Ar–H), 7.74 (dd, $^3J_{HH}$ 7.8, $^3J_{HH}$ 7.9, Ar–H), 7.78 (dd, $^3J_{HH}$ 8.0, $^3J_{HH}$ 8.1, 1H, Ar–H). ^{13}C $\{^1$H$\}$ NMR (100 MHz, CDCl$_3$): δ 24.9 (CH$_3$), 65.0 (CH$_2$), 65.1 (CH$_2$), 108.6 (C), 118.7 (CH), 121.7 (CH), 124.4 (CH), 129.1 (CH), 131.1 (CH), 135.3 (C), 137.5 (CH), 149.8 (C), 154.9 (C), 161.1 (C). IR (cm^{-1}): 1587 (C=N)$_{pyridine}$, 1530 (NO$_2$)$_{asymm}$, 1369 (NO$_2$)$_{symm}$ HRMS (TOFMS, ASAP): calcd for C$_{15}$H$_{15}$N$_2$O$_4$ [M + H]$^+$ 287.1032, found 287.1034.

Synthesis of 1-(6-(2-aminophenyl)pyridine-2-yl)ethanone

2-(2-Methyl-1,3-dioxolan-2-yl)-6-(2-nitrophenyl)pyridine (1.040 g, 3.6 mmol) and SnCl$_2$·2H$_2$O (8.220 g, 36.0 mmol) were suspended in bench ethanol (34 mL) and sonicated for 2 h, whereupon a bright yellow slurry was obtained. This slurry was concentrated under reduced pressure and partitioned between 1 M NaOH (100 mL) and CHCl$_3$ (100 mL) until a bright yellow organic phase was observed. The organic phase was separated and the aqueous phase washed with CHCl$_3$ (3 × 25 mL). The combined organic phases were washed with water (2 × 30 mL) and concentrated to a smaller volume under reduced pressure. Aqueous HCl (150 mL, 16% (v/v)) was added to the solution and the resultant biphase stirred for 1 h at ambient temperature. The reaction mixture was neutralised with K$_2$CO$_3$, the organic phase separated and the aqueous

phase washed with dichloromethane (2 × 30 mL). The combined organic extracts were washed with water (1 × 30 mL) and brine (1 × 30 mL) and then filtered through Celite layered with magnesium sulphate. The filtrate was concentrated under reduced pressure to afford 1-(6-(2-aminophenyl)pyridin-2-yl)-ethanone as a brown/yellow oil which slowly solidifies (0.68 g, 89%). Mp: 95–98 °C. ^{1}H NMR (400 MHz, CDCl$_3$): δ 2.73 (s, 3H, MeC═O), 5.77 (br, s, 2H, NH$_2$), 6.82 (m, 2H, Ar–H), 7.22 (ddd, $^3J_{HH}$ 7.3, $^3J_{HH}$ 8.1, $^4J_{HH}$ 1.6, 1H, Ar–H), 7.56 (dd, $^3J_{HH}$ 7.8, $^4J_{HH}$ 1.5, 1H, Ar–H), 7.85–7.95 (m, 3H, Py–H). ^{13}C{^{1}H} NMR (100 MHz, CDCl$_3$): δ 26.1 (Me–C═O), 117.4, 118.0, 119.0 (CH), 121.3 (C), 125.7 (CH), 129.6 (CH), 130.5 (CH), 137.9 (CH), 146.5 (C), 151.7 (C), 158.7 (C), 199.4 (C═O). IR (cm^{-1}): 3456, 3363 (NH), 1695 (C═O)$_{ketone}$, 1585 (C═N)$_{pyridine}$. ESIMS: m/z 213 [M + H]$^+$. HRMS (FAB): calcd for C$_{13}$H$_{13}$N$_2$O [M + H]$^+$ 213.10246, found 213.10252.

Synthesis of 2-(C$_6$H$_4$-2-NH$_2$)-6-(CMe═NAr)C$_5$H$_3$N (HL1)

(a) **Ar = 4-i-PrC$_6$H$_{34}$ (HL1a).** To a round bottomed flask equipped with stir bar was added 1-(6-(2-aminophenyl)pyridin-2-yl)ethanone (0.500 g, 2.4 mmol) and 4-isopropylaniline (2.070 g, 15.3 mmol). The reaction vessel was then lowered into a pre-heated heating mantle set at 225 °C and the mixture stirred for 15 min before a catalytic amount of glacial acetic acid was introduced. After 15 min at 225 °C the reaction vessel was allowed to cool to room temperature. The excess aniline was removed by distillation under reduced pressure, the resultant dark residue heated to reflux in ethanol (10 ml) and hot filtered. The filtrate was concentrated to half volume and allowed to cool to room temperature to yield HL1a as a yellow solid (0.040 g, 5%). Mp: 113–115 °C. ^{1}H NMR (400 MHz, CDCl$_3$): δ 1.28 (d, $^3J_{HH}$ 7.0, 6H, CHMe_2), 2.37 (s, 3H, MeC═N), 2.92 (sept, $^3J_{HH}$ 7.0, 1H, CHMe$_2$), 5.79 (br, s, 2H, NH$_2$), 6.76–6.84 (m, 4H, Ar–H), 7.20 (ddd, $^3J_{HH}$ 8.1, $^3J_{HH}$ 7.4, $^4J_{HH}$ 1.5, 1H, Ar–H), 7.23 (d, $^3J_{HH}$ 8.2, 2H, Ar–H), 7.58 (dd, $^3J_{HH}$ 7.8, $^3J_{HH}$ 1.5, 1H, Ar–H), 7.74 (dd, $^3J_{HH}$ 8.0, $^4J_{HH}$ 0.9, 1H, Py–H), 7.86 (dd, $^3J_{HH}$ 7.93, $^3J_{HH}$ 7.9, 1H, Py–H), 8.76 (dd, $^3J_{HH}$ 7.9, $^4J_{HH}$ 1.0, 1H, Py–H). ^{13}C{^{1}H} NMR (100 MHz, CDCl$_3$): δ 16.6 (MeC═N), 24.1 (CHMe_2), 33.6 (CHMe$_2$), 117.3, 117.9, 118.8, 119.3 (CH), 122.1 (C), 123.2 (CH), 126.9 (CH), 129.6 (CH), 130.1 (CH), 137.4 (CH), 144.2 (C), 146.5 (C), 148.8 (C), 155.2 (C), 158.2 (C), 166.5 (MeC═N). IR (cm^{-1}): 1635 (C═N)$_{imine}$, 1587 (C═N)$_{pyridine}$. ESIMS: m/z 330 [(M + H)]$^+$. HRMS (FAB): calcd C$_{22}$H$_{24}$N$_3$ [M + H]$^+$ 330.1970, found 330.1968.

(b) **Ar = 2,6-i-Pr$_2$C$_6$H$_3$ (HL1b).** Employing a similar procedure to that described for HL1a with 1-(6-(2-aminophenyl)-pyridin-2-yl)ethanone (0.700 g, 3.3 mmol), 2,6-diisopropyl-aniline (3.800 g, 21.5 mmol) gave following work-up HL1b as a yellow solid (0.54 g, 44%). Crystals suitable for an X-ray determination were grown by slow cooling of an ethanol solution containing the compound. Mp: 139–141 °C. ^{1}H NMR (400 MHz, CDCl$_3$): δ 1.14 (d, $^3J_{HH}$ 6.9, 6H, CHMe_2), 1.15 (d, $^3J_{HH}$ 7.0, 6H, CHMe_2), 2.21 (s, 3H, MeC═N), 2.75 (sept, $^3J_{HH}$ 6.9, 2H, CHMe$_2$), 5.72 (br, s, 2H, NH$_2$), 6.80 (dd, $^3J_{HH}$ 8.2, $^4J_{HH}$ 1.0, 1H, Ar–H), 6.82 (ddd, $^3J_{HH}$ 8.2, $^3J_{HH}$ 8.2, $^4J_{HH}$ 1.3, 1H, Ar–H), 7.08 (dd, $^3J_{HH}$ 8.7, $^3J_{HH}$ 6.3, 1H, Ar–H), 7.17 (dd, $^3J_{HH}$ 6.9,

$^3J_{HH}$ 8.5, 2H, Ar–H), 7.21 (ddd, $^3J_{HH}$ 7.3, $^3J_{HH}$ 8.0, $^4J_{HH}$ 1.5, 1H, Ar–H), 7.59 (dd, $^3J_{HH}$ 8.0, $^4J_{HH}$ 1.5, 1H, Ar–H), 7.78 (dd, $^3J_{HH}$ 8.0, $^3J_{HH}$ 0.9, 1H, Py–H), 7.90 (dd, $^3J_{HH}$ 7.9, $^3J_{HH}$ 7.9, 1H, Py–H), 8.26 (dd, $^3J_{HH}$ 7.8, $^4J_{HH}$ 0.9, 1H, Py–H). ^{13}C{^{1}H} NMR (100 MHz, CDCl$_3$): δ 17.5 (MeC═N), 22.9 (CHMe_2), 23.2 (CHMe_2), 28.3 (CHMe$_2$), 117.6, 118.2 (CH), 118.8 (C), 122.2 (CH), 123.0 (CH), 123.4 (CH), 123.7 (CH), 129.6 (CH), 130.1 (CH), 135.8 (C), 137.6 (CH), 146.1 (C), 146.3 (C), 154.5 (C), 158.2 (C), 165.0 (Me–C═N). IR (cm^{-1}): 3451, 3282 (br, NH), 1642 (C═N)$_{imine}$, 1584 (C═N)$_{pyridine}$. ESIMS: m/z 372 [(M + H)]$^+$. HRMS (FAB): calcd C$_{25}$H$_{30}$N$_3$O [M + H]$^+$ 372.24322, found 372.24310.

Synthesis of [{2-(C$_6$H$_4$-2-NH)-6-(CMe═NAr)}Pd(OAc)] (1)

(a) **Ar = 4-i-PrC$_6$H$_4$ (1a).** A Schlenk flask equipped with stir bar was evacuated and backfilled with nitrogen and loaded with Pd(OAc)$_2$ (0.740 g, 3.3 mmol), 1-(6-(2-aminophenyl)-pyridin-2-yl)ethanone (0.690 g, 0.81 mmol), 4-isopropylaniline (0.660 g, 4.9 mmol) and toluene (70 mL). The reaction vessel was stirred and heated to 80 °C for 3 h. The resultant green/brown solution was evaporated and the resultant solid dissolved in the minimum volume of chloroform before hexane was added to precipitate 1a as a green/brown solid (1.45 g, 89%). Crystals suitable for an X-ray determination were grown by slow diffusion of hexane into a solution of 1a in CHCl$_3$ at room temperature. Mp: >260 °C. ^{1}H NMR (400 MHz, CDCl$_3$): δ 1.22 (d, $^3J_{HH}$ 6.9, 6H, CHMe_2), 1.53 (s, 3H, –OC(O)Me), 2.33 (s, 3H, MeC═N), 2.98 (sept, $^3J_{HH}$ 6.9, 1H, CHMe$_2$), 5.60 (br, s, 1H, NH), 6.42 (ddd, $^3J_{HH}$ 6.6, $^3J_{HH}$ 8.5, $^4J_{HH}$ 1.2, 1H, Ar–H), 6.86 (dd, $^3J_{HH}$ 8.5, $^4J_{HH}$ 1.2, 1H, Ar–H), 7.02 (ddd $^3J_{HH}$ 6.6, $^3J_{HH}$ 7.9, $^4J_{HH}$ 1.4, 1H, Ar–H), 7.07 (d, $^3J_{HH}$ 8.4, 2H, Ar–H), 7.23 (d, $^3J_{HH}$ 8.3, 2H, Ar–H), 7.59 (dd, $^3J_{HH}$ 7.4, $^4J_{HH}$ 1.0, 1H, Py–H), 7.89 (d, $^3J_{HH}$ 8.0, 1H, Ar–H), 7.99 (dd, $^3J_{HH}$ 7.4, $^3J_{HH}$ 8.8, 1H, Py–H), 8.56 (d, $^3J_{HH}$ 8.8, 1H, Py–H). ^{13}C{^{1}H} NMR (100 MHz, CDCl$_3$): δ 16.3 (MeC═N), 21.9 (MeCO$_2$), 22.9 (CHMe_2), 32.9 (CHMe$_2$), 111.8 (CH), 112.9 (C), 119.7 (CH), 121.5 (CH), 122.0 (CH), 125.4 (CH), 125.6 (CH), 128.3 (CH), 129.1 (CH), 133.5 (CH), 141.7 (C), 146.9 (C), 148.5 (C), 148.8 (C), 152.7 (C), 169.5 (Me–C═N), 177.0 (Me–CO$_2$). IR (cm^{-1}): 1600 (C═N)$_{imine}$, 1591 (COO$_{asymm}$/C═N$_{pyridine}$), 1367 (COO)$_{symm}$ FABMS: m/z 493 [M]$^+$, 433 [M − OAc]$^+$. Anal Calc. for (C$_{24}$H$_{25}$N$_3$O$_2$Pd): C, 58.36; H, 5.10; N, 8.51. Found: C, 58.26; H, 5.23; N, 8.51%.

(b) **Ar = 2,6-i-Pr$_2$C$_6$H$_3$ (1b).** A Schlenk flask equipped with stir bar was evacuated and backfilled with nitrogen and loaded with Pd(OAc)$_2$ (0.180 g, 0.81 mmol), HL1b (0.300 g, 0.81 mmol) and toluene (30 mL). After stirring at 60 °C overnight, the green reaction mixture was cooled to room temperature and filtered through Celite and the Celite cake washed thoroughly with dichloromethane. The filtrate was concentrated to ca. 1 mL whereupon hexane (20 mL) was added. The resulting green precipitate was filtered and dried under reduced pressure forming 1b as a dark green powder (0.38 g, 88%). Crystals suitable for an X-ray diffraction study could be grown by slow diffusion of hexane into a chloroform solution of the complex at room temperature. Mp: >260 °C. ^{1}H NMR (400 MHz, CDCl$_3$): δ 1.14 (d, $^3J_{HH}$ 6.8, 6H, CHMe_2), 1.39

(d, $^3J_{HH}$ 6.8, 6H CHMe_2), 1.51 (s, 3H, –OC(O)Me), 2.41 (s, 3H, MeC=N), 3.14 (sept, $^3J_{HH}$ 6.8, 2H, CHMe$_2$), 6.53 (ddd, $^3J_{HH}$ 8.6, $^3J_{HH}$ 6.5, $^4J_{HH}$ 1.4, 1H, Ar–H), 7.06 (dd, $^3J_{HH}$ 8.5, $^4J_{HH}$ 1.2, 1H, Ar–H), 7.13 (ddd, $^3J_{HH}$ 8.5, $^3J_{HH}$ 6.4, $^4J_{HH}$ 1.4, 1H, Ar–H), 7.26 (m, 2H, Ar–H), 7.36 (dd, $^3J_{HH}$ 8.7, $^3J_{HH}$ 6.8, 1H, Ar–H), 7.39 (br, s, 1H, NH), 7.82 (dd $^3J_{HH}$ 7.4, $^4J_{HH}$ 1.0, 1H, Py–H), 8.01 (d, $^3J_{HH}$ 8.6, 1H, Ar–H), 8.10 (dd, $^3J_{HH}$ 8.8, $^3J_{HH}$ 7.3, 1H, Py–H), 6.80 (d, $^3J_{HH}$ 8.7, 1H, Py–H). ^{13}C{^{1}H} NMR (100 MHz, CDCl$_3$): δ 17.0 (CHMe_2), 22.3 (CHMe_2), 22.7 (MeCO$_2$), 22.8 (MeC=N), 27.6 (CHMe$_2$), 112.0 (CH), 112.6 (C), 120.3 (CH), 121.0 (CH), 122.4 (CH), 125.7 (CH), 126.7 (CH), 127.7 (CH), 129.2 (CH), 132.5 (CH), 139.0 (C), 139.4 (C), 149.0 (C), 149.2 (C), 152.7 (C), 170.1 (Me–C=N), 177.2 (Me–CO$_2$). IR (cm^{-1}): 1614 (C=N)$_{imine}$, 1583 (COO)$_{asymm}$/C=N$_{pyridine}$), 1367 (COO)$_{symm}$ ESIMS: m/z 476 [M – OAc]$^+$. TOFMS (ASAP): m/z 536 [M$^+$], 476 [M – OAc]$^+$. Anal Calc. for (C$_{28}$H$_{32}$Cl$_3$N$_3$O$_2$Pd): C, 51.32; H, 4.92; N, 6.41. Found: C, 50.92; H, 4.18; N, 7.36%.

Synthesis of [{2-(C$_6$H$_4$-2-NH)-6-(CMe=NAr)}PdCl] (2)

(a) Ar = 4-i-PrC$_6$H$_4$ (2a). A round bottomed flask equipped with stir bar and open to the air was loaded with **1a** (0.595 g, 1.20 mmol), dichloromethane (5 mL) and brine (5 mL). The reaction mixture was stirred rapidly for 1 h at room temperature whereupon both phases were diluted and the aqueous layer removed *via* a separating funnel. The organic phase was washed with water (2 × 20 mL) and concentrated to a smaller volume under reduced pressure. The dark green solution was filtered through a Celite plug and the plug washed thoroughly with dichloromethane. All volatiles were removed under reduced pressure affording **2a** as a dark brown solid (0.56 g, 99%). Single crystals suitable an X-ray determination were grown by diffusion of hexane into a solution of **2a** in chloroform at room temperature. Mp: >260 °C. ^{1}H NMR (400 MHz, CDCl$_3$): δ 1.23 (d, $^3J_{HH}$ 6.9, 6H, CHMe_2), 2.28 (s, 3H, MeC=N), 2.89 (sept, $^3J_{HH}$ 6.9, 1H, CHMe$_2$), 5.59 (br, s, 1H, NH), 6.43 (ddd, $^3J_{HH}$ 6.1, $^3J_{HH}$ 8.0, $^4J_{HH}$ 1.20, 1H, Ar–H), 6.81 (dd, $^3J_{HH}$ 8.6, $^4J_{HH}$ 1.0, 1H, Ar–H), 6.99–7.03 (m, 5H, Ar–H), 7.19 (d, $^3J_{HH}$ 8.2, 2H, Ar–H), 7.55 (dd, $^3J_{HH}$ 7.5, $^4J_{HH}$ 0.9, 1H, Py–H), 7.73–7.79 (m, 2H, Py–H/Ar–H), 8.30 (d, $^3J_{HH}$ 8.7, 1H, Py–H). ^{13}C{^{1}H} NMR (125 MHz, CDCl$_3$): δ 17.0 (CH$_3$C=N), 22.9 (CHMe_2), 32.7 (CHMe$_2$), 112.1 (CH), 112.8 (C), 119.7 (CH), 121.6 (CH), 122.3 (CH), 125.1 (CH), 125.5 (CH), 128.2 (CH), 129.5 (CH), 133.4 (CH), 142.9 (C), 146.6 (C), 148.4 (C), 148.4 (C), 153.1 (C), 171.0 (Me–C=N). IR (cm^{-1}): 1603 (C=N)$_{imine}$, 1576 (C=N)$_{pyridine}$. FABMS: m/z 469 (M)$^+$, 434 (M–Cl)$^+$. Anal Calc. for (For C$_{22}$H$_{22}$ClN$_3$Pd): C, 56.18; H, 4.71; N, 8.93. Found: C, 56.11; H, 4.69; N, 9.00%.

(b) Ar = 2,6-i-Pr$_2$C$_6$H$_3$ (2b). Employing a similar procedure to that described for **2a** using **1b** (0.544 g, 1.02 mmol) gave **2b** as a dark green solid (0.520 g, 99%). Single crystals suitable for an X-ray diffraction study could be grown by slow diffusion of hexane into a chloroform solution of **2b** at room temperature. Mp: >260 °C. ^{1}H NMR (400 MHz, CDCl$_3$): δ 1.05 (d, $^3J_{HH}$ 6.9, 6H, CHMe_2), 1.35 (d, $^3J_{HH}$ 6.9, 6H, CHMe_2), 2.28 (s, 3H, MeC=N), 2.99 (sept, $^3J_{HH}$ 6.9, 2H, CHMe$_2$), 5.91 (br, s, 1H, NH), 6.49 (ddd, $^3J_{HH}$ 8.5, $^3J_{HH}$ 6.7, $^4J_{HH}$ 1.3, 1H, Ar–H), 6.92

(dd, $^3J_{HH}$ 8.6, $^4J_{HH}$ 1.2, 1H, Ar–H), 7.06 (ddd, $^3J_{HH}$ 8.2, $^3J_{HH}$ 6.5, $^4J_{HH}$ 1.4, Ar–H), 7.19 (m, 2H, Ar–H), 7.28 (dd, $^3J_{HH}$ 8.5, $^3J_{HH}$ 8.5, 1H, Ar–H), 7.77 (dd, $^3J_{HH}$ 7.3, $^4J_{HH}$ 1.1, 1H, Py–H), 7.92 (dd, $^3J_{HH}$ 8.6, $^4J_{HH}$ 1.5, 1H, Ar–H), 8.06 (dd, $^3J_{HH}$ 8.8, $^3J_{HH}$ 8.4, 1H, Py–H), 8.63 (d, $^3J_{HH}$ 8.6, 1H, Py–H). ^{13}C {^{1}H} NMR (125 MHz, CDCl$_3$): δ 18.0 (Me–C=N), 23.7 (CHMe_2), 23.8 (CHMe_2), 28.7 (CHMe$_2$), 113.6 (CH), 113.8 (C), 121.3 (CH), 122.1 (CH), 123.6 (CH), 127.2 (CH), 128.1 (CH), 129.1 (CH), 130.8 (CH), 134.1 (CH), 139.7 (C), 141.6 (C), 150.0 (C), 150.3 (C), 153.7 (C), 172.1 (Me–C=N). IR (cm^{-1}): 1608 (C=N)$_{imine}$, 1577 (C=N)$_{pyridine}$. FABMS: m/z 511 [M + H]$^+$, 475 [M – Cl]$^+$. Anal Calc. for (C$_{25}$H$_{28}$ClN$_3$Pd): C, 58.60; H, 5.51; N, 8.20. Found: C, 58.49; H, 5.35; N, 8.26%.

Synthesis of [{2-(C$_6$H$_4$-2-NH)-6-(CMe=NAr)}Pd(C$_6$H$_5$)] (3)

(a) Ar = 4-i-PrC$_6$H$_4$ (3a). A Schlenk flask equipped with stir bar was evacuated and backfilled with nitrogen and loaded with **2a** (0.208 g, 0.44 mmol) and THF (20 mL). The reaction mixture was stirred and cooled to −78 °C for 15 min. A solution of PhLi (861 μL, 1.55 mmol, 1.8 M in n-Bu$_2$O) was added slowly and the reaction mixture stirred at −78 °C for a further 2 h. One drop of water was added and the solution slowly warmed to room temperature. All volatiles were removed under reduced pressure and the resultant green solid re-dissolved in dichloromethane (20 mL) and washed with water (2 × 20 mL) and brine (10 mL). Following drying over anhydrous magnesium sulphate and filtration, the resulting green solution was concentrated to a smaller volume (ca. 5 mL) and hexane added to precipitate **3a** as a green solid (0.161 g, 71%). Single crystals suitable for an X-ray determination were obtained by slow diffusion of hexane into a solution of **3a** in chloroform at room temperature. ^{1}H NMR (400 MHz, CDCl$_3$): δ 1.19 (d, $^3J_{HH}$ 6.9, 6H, CHMe_2), 2.46 (s, 3H, MeC=N), 2.80 (sept, $^3J_{HH}$ 6.9, 1H, CHMe$_2$), 5.48 (br, s, 1H, NH), 6.44 (ddd, $^3J_{HH}$ 6.5, $^3J_{HH}$ 8.0, $^4J_{HH}$ 1.1, 1H, Ar–H), 6.65 (d, $^3J_{HH}$ 8.4, 2H, Ar–H), 6.73–6.75 (m, 3H, Ar–H), 6.90 (dd, $^3J_{HH}$ 8.6, $^4J_{HH}$ 1.3, 1H, Ar–H), 6.95 (d, $^3J_{HH}$ 8.4, 2H, Ar–H), 7.05 (ddd, $^3J_{HH}$ 6.6, $^3J_{HH}$ 8.1, $^4J_{HH}$ 1.4, 1H, Ar–H), 7.07–7.09 (m, 2H, Ar–H), 7.82 (d, $^3J_{HH}$ 7.1, 1H, Py–H), 7.98 (dd, $^3J_{HH}$ 8.5, $^4J_{HH}$ 1.3, 1H, Ar–H), 8.05 (dd, $^3J_{HH}$ 7.5, $^3J_{HH}$ 8.6, 1H, Py–H), 8.58 (d, $^3J_{HH}$ 8.8, 1H, Py–H). ^{13}C{^{1}H} NMR (100 MHz, CDCl$_3$) δ 18.3 (Me–C=N), 24.0 (CHMe_2), 33.7 (CHMe$_2$), 111.9 (CH), 114.0 (C), 121.3 (CH), 122.2 (CH), 122.6 (CH), 122.9 (CH), 125.9 (CH), 126.0 (CH), 126.1 (CH), 129.9 (CH), 130.0 (CH), 134.2 (CH), 135.9 (CH), 145.1, 146.9, 152.0, 152.1, 153.1, 158.5 (C), 170.5 (MeC=N). IR (cm^{-1}): 1602 (C=N)$_{imine}$, 1567 (C=N)$_{pyridine}$. FABMS: m/z 511 [M]$^+$. Anal Calc. for (C$_{28}$H$_{27}$N$_3$Pd·1.5OH$_2$): C, 62.40; H, 5.61; N, 7.80. Found: C, 62.04; H, 5.33; N, 8.16%.

(b) Ar = 2,6-i-Pr$_2$C$_6$H$_3$ (3b). A Schlenk flask equipped with stir bar was evacuated and backfilled with nitrogen and loaded with **HL1b** (0.100 g, 0.13 mmol), NaH (0.052 g, 2.20 mmol) and THF (10 mL). The resulting slurry was stirred and heated to reflux for 72 h before being allowed to cool to room temperature. The reaction mixture was transferred by cannular filtration to a second Schlenk flask containing [[(PPh$_3$)$_2$PdPh(Br)]] (0.100 g, 0.13 mmol) and the contents stirred and heated to

reflux for a further 72 h. On cooling to room temperature, the resulting green solution was concentrated under reduced pressure and re-dissolved in chloroform (10 mL) before being filtered through a Celite plug. All volatiles were removed under reduced pressure and the resulting residue triturated with hexane (3 × 20 mL) and **3b** collected as a green solid (0.067 g, 93%). Crystals suitable for an X-ray determination were grown by slow diffusion of hexane into a solution of **3b** in chloroform at room temperature. ^{1}H NMR (400 MHz, CDCl$_3$): δ 0.90 (d, [3]J_{HH} 6.7, 6H, CHMe_2), 0.95 (d, [3]J_{HH} 6.8, 6H, CHMe_2), 2.32 (s, 3H, MeC=N), 2.94 (sept, [3]J_{HH} 6.8, 2H, CHMe$_2$), 6.40 (ddd, [3]J_{HH} 8.1, [3]J_{HH} 6.6, [4]J_{HH} 1.3, 1H, Ar–H), 6.66–6.73 (m, 3H, Ar–H), 6.84 (dd, [3]J_{HH} 8.4, [4]J_{HH} 1.2, 1H, Ar–H), 6.88–6.93 (m, 2H, Ar–H), 6.99 (ddd, [3]J_{HH} 8.3, [3]J_{HH} 6.6, [4]J_{HH} 1.6, 1H, Ar–H), 6.99 (d, [3]J_{HH} 7.8, 2H, Ar–H), 7.12 (dd, [3]J_{HH} 7.7, [3]J_{HH} 7.7, 1H, Ar–H), 7.80 (dd, [3]J_{HH} 7.5, [4]J_{HH} 1.0, 1H, PyH), 7.91 (dd, [3]J_{HH} 8.6, [4]J_{HH} 1.4, 1H, Ar–H), 8.02 (dd, [3]J_{HH} 8.8, [3]J_{HH} 7.5, 1H, Py–H), 8.55 (d, [3]J_{HH} 8.7, 1H, Py–H). ^{13}C{^{1}H} NMR (100 MHz, CDCl$_3$): δ 19.3 (MeC=N), 22.9 (CHMe_2), 24.2 (CHMe_2), 28.2 (CHMe$_2$), 112.1 (CH), 114.5 (C), 121.3 (C), 122.5 (CH), 122.8 (CH), 123.5 (CH), 125.8 (CH), 126.5 (CH), 127.1 (CH), 130.0 (CH), 130.1 (CH), 134.3 (CH), 135.9 (CH), 139.5 (CH), 142.9 (C), 151.5 (C), 152.4 (C), 153.2 (C), 155.5 (C), 172.1 (Me–C=N). IR (cm^{-1}): 1605 (C=N)$_{imine}$, 1571 (C=N)$_{pyridine}$. FABMS: m/z 553 [M + H]$^+$.

Synthesis of [{2-(C$_6$H$_4$-2-NH)-6-(CMe=N(4-i-PrC$_6$H$_4$)}Pd-(NCMe)][X] (4 and 5)

(a) X = BF$_4$ (4). A Schlenk flask equipped with stir bar was evacuated and backfilled with nitrogen and loaded with **2a** (0.200 g, 0.426 mmol), AgBF$_4$ (0.083 g, 0.426 mmol) and MeCN (20 mL). The reaction mixture was stirred at room temperature for 12 h, at which point the suspension was allowed to settle and the solution transferred by cannula filtration into another Schlenk flask. All volatiles were removed under reduced pressure to afford **4** as a dark green solid (0.233 g, 97%). Mp: >260 °C. ^{1}H NMR (400 MHz, CD$_3$CN): δ 1.21 (d, [3]J_{HH} 6.9, 3H, CHMe_2), 2.27 (s, 3H, CH$_3$C=N), 2.93 (sept, [3]J_{HH} 6.9, 1H, CHMe$_2$), 6.60 (dd, [3]J_{HH} 7.5, [3]J_{HH} 7.5, 1H, Ar–H), 6.98 (d, [3]J_{HH} 8.4, 1H, Ar–H), 7.04 (d, [3]J_{HH} 7.8, 2H, Ar–H), 7.10 (dd, [3]J_{HH} 7.6, [3]J_{HH} 7.8, 1H, Ar–H), 7.34 (d, [3]J_{HH} 8.0, 2H, Ar–H), 7.83 (d, [3]J_{HH} 7.5, 1H, Py–H), 7.89 (d, [3]J_{HH} 8.0, 1H, Ar–H), 8.08 (dd, [3]J_{HH} 8.0, [3]J_{HH} 8.0, 1H, Py–H), 8.53 (d, [3]J_{HH} 8.6, 1H, Py–H), the co-ordinated CH$_3$CN ligand was not observed due to rapid exchange with bulk CD$_3$CN. ^{13}C{^{1}H} NMR (100 MHz, CD$_3$CN): δ 17.0 (CH$_3$C=N), 22.9 (CHMe_2), 33.3 (CHMe$_2$), 115.3 (CH), 117.0 (C), 119.6 (CH), 122.3 (CH), 124.9 (CH), 126.9 (CH), 127.0 (CH), 129.7 (CH), 131.2 (CH), 136.8 (CH), 142.9 (C), 147.1 (C), 148.8 (C), 149.5 (C), 155.0 (C), 174.8 (C=N). ^{19}F{^{1}H} NMR (375 MHz, CD$_3$CN): δ −151 (-BF$_4$). ESIMS (+ve) m/z: 475 [M − BF$_4$]$^+$; ESIMS (−ve): m/z 87 [BF$_4$]$^-$. Anal Calc. for (C$_{24}$H$_{25}$N$_4$F$_4$PdB): C, 51.23; H, 4.48; N, 9.96. Found: C, 51.13; H, 4.40; N, 9.87%.

(b) X = O$_3$SCF$_3$ (5). Employing a similar procedure to that described for **4** using **2a** (0.205 g, 0.44 mmol), AgOSO$_2$CF$_3$ (0.112 g, 0.44 mmol) and MeCN (20 mL) gave **5** as a dark green solid (0.259 g, 95%). Crystallisation by slow diffusion of

petroleum ether (40–60) into a solution of the salt in aceto-nitrile–dichloromethane (5 : 95) gave **5** as a microcrystalline powder. Single crystals of pyridine-containing **5′** suitable for X-ray diffraction could be obtained by slow diffusion of hexane into a chloroform solution of **5** that contained a few drops of pyridine. Complex **5**: Mp: >260 °C. ^{1}H NMR (400 MHz, CD$_3$CN): δ 1.32 (d, [3]J_{HH} 6.9, 6H, CHMe_2), 2.51 (s, 3H, MeC=N), 3.05 (sept, [3]J_{HH} 6.9, 1H, CHMe$_2$), 6.14 (br, s, 1H, NH), 6.74 (app. t, [3]J_{HH} 7.7, 1H, Ar–H), 7.17–7.23 (m, 3H, Ar–H), 7.26–7.29 (m, 1H, Ar–H), 7.48 (d, [3]J_{HH} 8.3, 2H, Ar–H), 8.16 (m, 2H, Ar–H), 8.33 (dd, [3]J_{HH} 8.0, [3]J_{HH} 8.0, 1H, Py–H), 8.54 (d, [3]J_{HH} 8.5, 1H, Py–H), the coordinated CH$_3$CN ligand was not observed due to rapid exchange with bulk CD$_3$CN. ^{13}C{^{1}H} NMR (100 MHz, CD$_3$CN): δ 17.0 (MeC=N), 22.9 (CHMe_2), 33.3 (CHMe$_2$), 115.4 (CH), 119.2 (C), 119.7 (CH), 122.4 (CH), 124.9 (CH), 126.9 (CH), 129.7 (CH), 131.0 (CH), 136.7 (CH), 142.8 (C), 146.7 (C), 148.8 (C), 149.3 (C), 154.8 (C), 174.7 (MeC=N), CF$_3$SO$_3$$^-$ not observed. ^{19}F{^{1}H} NMR (375 MHz, CD$_3$CN): δ −79 (O$_3$SCF$_3$). IR (cm^{-1}): 1602 (C=N)$_{imine}$, 1570 (C=N)$_{pyridine}$. ESIMS (+ve): m/z 475 [M − O$_3$SCF$_3$]$^+$; ESIMS (−ve): m/z: 149 [O$_3$SCF$_3$]$^-$. Anal Calc. for (C$_{25}$H$_{25}$N$_4$O$_3$F$_3$PdS·CH$_2$Cl$_2$): C, 43.99; H, 3.83; N, 7.89. Found: C, 44.13; H, 3.78; N, 7.60%.

Reaction of 3a with Selectfluor in NMR tube at reduced temperatures

(a) −40 to 0 °C. Complex **3a** (0.005 g, 0.0098 mmol) and Selectfluor™ (0.0035 g, 0.0098 mmol) were loaded into a Young's NMR tube open to the air and then cooled to −100 °C before acetonitrile-d_3 was added and the system sealed. The NMR tube was inserted into a 400 MHz NMR spectrometer pre-cooled to −40 °C and the ^{19}F and ^{1}H NMR spectra were recorded at −40 °C and then at 10 °C intervals up to 0 °C. At −40 °C, ^{1}H NMR (400 MHz, CD$_3$CN): δ 1.16 (d, [3]J_{HH} 6.8, 6H, CHMe_2), 2.40 (s, 3H, MeC=N), 2.82 (sept, [3]J_{HH} 6.8, 1H, CHMe$_2$), 6.70 (d, [3]J_{HH} 8.5, 2H, Ar–H), 6.72–6.77 (m, 2H, Ar–H), 6.84–6.86 (m, 2H, Ar–H), 7.04 (d, [3]J_{HH} 8.4, 2H, Ar–H), 7.36–7.43 (m, 2H, Ar–H), 7.47–7.55 (m, 2H, Ar–H), 7.86 (dd, [3]J_{HH} 7.7, [4]J_{HH} 1.9, 1H, Ar–H), 8.17 (m, 1H, Ar–H), 8.40 (m, 2H, Ar–H). ^{19}F{^{1}H} NMR (375 MHz, CD$_3$CN): δ −152 (BF$_4$), −172 (HF). At −30 °C, ^{1}H NMR δ no change. ^{19}F{^{1}H} NMR: δ −152 (BF$_4$), −172 (HF). At −20 °C, ^{1}H NMR δ no change. ^{19}F{^{1}H} NMR: δ −152 (BF$_4$), −173 (HF). At −10 °C, ^{1}H NMR δ no change. ^{19}F{^{1}H} NMR: δ −152 (BF$_4$), −173 (HF). At 0 °C: ^{1}H NMR δ no change. ^{19}F{^{1}H} NMR: δ −152 (8F, BF$_4$), −174 (1F, HF).

(b) 0 °C to room temperature. The reaction mixture prepared in (a) was further warmed to room temperature and the ^{1}H NMR spectrum recorded periodically. After 48 h, complete conversion to **4** (data as reported for **4** above) and biphenyl was observed. ^{19}F{^{1}H} NMR δ −152 (BF$_4$), −181 (HF).

Crystallographic studies

Data for HL1b, 1a, 1b, 2a, 2b, 3a, 3b and 5′ were collected on a Bruker APEX 2000 CCD diffractometer. Details of data collection, refinement and crystal data are listed in Table 6. The data were corrected for Lorentz and polarisation effects and empiri-

Table 6 Crystallographic and data processing parameters for HL1b, 1a, 1b, 2a, 2b, 3a, 3b and 5$'^{a}$

Complex	HL1b	1a	1b	2a
Formula	$C_{25}H_{29}N_3$	$C_{24}H_{25}Cl_3N_3O_2Pd \cdot CHCl_3 \cdot OH_2$	$C_{28}H_{32}Cl_3N_3O_2Pd$	$C_{22}H_{22}ClN_3Pd$
M	371.51	631.25	655.32	470.28
Crystal size (mm³)	0.24 × 0.17 × 0.12	0.27 × 0.05 × 0.04	0.27 × 0.17 × 0.11	0.23 × 0.20 × 0.04
Temperature (K)	150(2)	150(2)	150(2)	150(2)
Crystal system	Orthorhombic	Triclinic	Triclinic	Monoclinic
Space group	$Pbca$	$P\bar{1}$	$P\bar{1}$	$P2(1)/n$
a (Å)	12.906(10)	6.9770(16)	14.194(4)	17.674(4)
b (Å)	8.308(6)	12.184(3)	15.316(4)	8.9111(19)
c (Å)	39.43(3)	15.543(4)	15.711(4)	24.267(5)
α (°)	90	87.923(4)	61.002(5)	90
β (°)	90	84.029(5)	77.050(7)	93.133(5)
γ (°)	90	84.203(5)	80.162(7)	90
U (Å³)	4228(5)	1307.0(5)	2903.6(14)	3816.2(14)
Z	8	2	4	8
D_c (Mg m⁻³)	1.167	1.604	1.499	1.637
$F(000)$	1600	640	1336	1904
μ(Mo-K$_\alpha$)(mm⁻¹)	0.069	1.049	0.945	1.124
Reflections collected	28 600	10 332	22 854	28 912
Independent reflections	3715	5074	11 293	7469
R_{int}	0.2201	0.1059	0.1479	0.1336
Restraints/parameters	0/258	20/319	0/679	1/493
Final R indices ($I > 2\sigma(I)$)	$R_1 = 0.0628$ wR$_2$ = 0.1155	$R_1 = 0.0683$ wR$_2$ = 0.1067	$R_1 = 0.0873$ wR$_2$ = 0.1788	$R_1 = 0.0582$ wR$_2$ = 0.0914
All data	$R_1 = 0.1397$ wR$_2$ = 0.1377	$R_1 = 0.1235$ wR$_2$ = 0.1232	$R_1 = 0.1888$ wR$_2$ = 0.2173	$R_1 = 0.1237$ wR$_2$ = 0.1078
Goodness of fit on F^2 (all data)	0.871	0.861	0.848	0.890

Complex	2b	3a	3b	5′
Formula	$C_{26}H_{29}Cl_4N_3Pd$	$C_{28}H_{27}N_3Pd$	$C_{31}H_{33}N_3Pd$	$C_{28}H_{26}F_3N_4O_3PdS \cdot 2CHCl_3$
M	631.72	511.93	554.00	900.72
Crystal size (mm³)	0.36 × 0.31 × 0.04	0.26 × 0.12 × 0.05	0.25 × 0.22 × 0.10	0.46 × 0.14 × 0.04
Temperature (K)	150(2)	150(2)	150(2)	150(2)
Crystal system	Monoclinic	Monoclinic	Orthorhombic	Triclinic
Space group	$P2(1)/n$	$P2(1)/c$	$Pbca$	$P\bar{1}$
a (Å)	11.410(8)	17.244(11)	12.118(3)	14.155(7)
b (Å)	17.663(13)	11.142(8)	10.844(3)	16.226(8)
c (Å)	12.991(9)	12.238(8)	40.250(10)	17.503(8)
α (°)	90	90	90	89.109(9)
β (°)	94.182(13)	105.925(14)	90	76.364(11)
γ (°)	90	90	90	70.267(10)
U (Å³)	2611(3)	2261(3)	5289(2)	3668(3)
Z	4	4	8	4
D_c (Mg m⁻³)	1.607	1.504	1.391	1.631
$F(000)$	1280	1048	2288	1804
μ(Mo-K$_\alpha$)(mm⁻¹)	1.141	0.842	1.391	1.053
Reflections collected	19 939	17 292	41 613	26 756
Independent reflections	5116	4444	5763	12 826
R_{int}	0.0775	0.2311	0.0699	0.2649
Restraints/parameters	0/312	0/292	0/321	749/889
Final R indices ($I > 2\sigma(I)$)	$R_1 = 0.0446$ wR$_2$ = 0.0904	$R_1 = 0.0732$ wR$_2$ = 0.1210	$R_1 = 0.0431$ wR$_2$ = 0.0906	$R_1 = 0.1055$ wR$_2$ = 0.2112
All data	$R_1 = 0.0615$ wR$_2$ = 0.0955	$R_1 = 0.1615$ wR$_2$ = 0.1450	$R_1 = 0.0569$ wR$_2$ = 0.0955	$R_1 = 0.2711$ wR$_2$ = 0.2821
Goodness of fit on F^2 (all data)	1.044	0.867	1.122	0.829

^{a} Data in common: graphite-monochromated Mo-K$_\alpha$ radiation, λ = 0.71073 Å; $R_1 = \sum ||F_o| - |F_c||/\sum |F_o|$, wR$_2 = [\sum w(F_o^2 - F_c^2)^2/\sum w(F_o^2)^2]^{1/2}$, w$^{-1} = [\sigma^2(F_o)^2 + (aP)^2]$, $P = [\max(F_o^2, 0) + 2(F_c^2)]/3$, where a is a constant adjusted by the program; goodness of fit = $[\sum(F_o^2 - F_c^2)2/(n - p)]^{1/2}$ where n is the number of reflections and p the number of parameters.

cal absorption corrections applied. Structure solution by direct methods and structure refinement based on full-matrix least-squares on F^2 employed SHELXTL version 6.10.[21] Hydrogen atoms were included in calculated positions (C–H = 0.96–1.00 Å) riding on the bonded atom with isotropic displacement parameters set to 1.5 U_{eq}(C) for methyl H atoms and 1.2 U_{eq}(C) for all other H atoms. All non-H atoms were refined with anisotropic displacement parameters.

Acknowledgements

References

1 For reviews, see (*a*) A. J. Hickman and M. S. Sanford, *Nature*, 2012, **484**, 177–185; (*b*) L. M. Mirica and J. R. Khusnutdinova, *Coord. Chem. Rev.*, 2013, **257**, 299–314; (*c*) D. C. Powers and T. Ritter, *Top. Organomet. Chem.*, 2011, **503**, 129–156.

2 (*a*) D. C. Powers and T. Ritter, *Nat. Chem.*, 2009, **1**, 302–309; (*b*) F. Tang, F. Qu, J. R. Khusnutdinova, N. P. Rath and L. M. Mirica, *Dalton Trans.*, 2012, **41**, 14046–14050; (*c*) J. R. Khusnutdinova, N. P. Rath and L. M. Mirica, *J. Am. Chem. Soc.*, 2010, **132**, 7303–7305; (*d*) J. R. Khusnutdinova, N. P. Rath and L. M. Mirica, *J. Am. Chem. Soc.*, 2012, **134**, 2414–2422; (*e*) A. J. Canty, A. Ariafard, M. S. Sanford and B. F. Yates, *Organometallics*, 2013, **32**, 544–555; (*f*) M. D. Lotz, M. S. Remy, D. B. Lao, A. Ariafard, B. F. Yates, A. J. Canty, J. M. Mayer and M. L. Sanford, *J. Am. Chem. Soc.*, 2014, **136**, 8237–8242.

3 (*a*) J. R. Brandt, E. Lee, G. B. Boursalian and T. Ritter, *Chem. Sci.*, 2014, **5**, 169–179; (*b*) K. L. Hull, W. Q. Anani and M. S. Sanford, *J. Am. Chem. Soc.*, 2006, **128**, 7134; (*c*) N. D. Ball and M. S. Sanford, *J. Am. Chem. Soc.*, 2009, **131**, 3796–3797; (*d*) X. Wang, T.-S. Mei and J.-Q. Yu, *J. Am. Chem. Soc.*, 2009, **131**, 7520–7521; (*e*) K. M. Engle, T.-S. Mei, X. Wang and J.-Q. Yu, *Angew. Chem., Int. Ed.*, 2011, **50**, 1478–1491.

4 (*a*) T. Furuya and T. Ritter, *J. Am. Chem. Soc.*, 2008, **130**, 10060–10061; (*b*) T. Furuya, D. Benitez, E. Tkatchouk, A. E. Strom, P. Tamg, W. A. Goddard III and T. Ritter, *J. Am. Chem. Soc.*, 2010, **132**, 3793–3807; (*c*) T. Furuya, H. M. Kaiser and T. Ritter, *Angew. Chem., Int. Ed.*, 2008, **47**, 5993–5996; (*d*) E. Lee, A. S. Kamlet, D. C. Powers, C. N. Neumann, G. B. Boursalian, T. Furuya, D. C. Choi, J. M. Hooker and T. Ritter, *Science*, 2011, **334**, 639–642.

5 N. D. Ball and M. S. Sanford, *J. Am. Chem. Soc.*, 2009, **131**, 3796–3797.

6 A. R. Mazzotti, M. G. Campbell, P. Tang, J. M. Murphy and T. Ritter, *J. Am. Chem. Soc.*, 2013, **135**, 14012–14015.

7 (*a*) M. G. Campbell, S.-L. Zheng and T. Ritter, *Inorg. Chem.*, 2013, **52**, 13295–13297; (*b*) M. C. Campbell, D. C. Powers, J. Raynaud, M. J. Graham, P. Xie, E. Lee and T. Ritter, *Nat. Chem.*, 2011, **473**, 470–477.

8 (*a*) V. V. Grushin and W. J. Marshall, *J. Am. Chem. Soc.*, 2006, **128**, 4632–4641; (*b*) D. J. Cardenas, B. Martin-Matute

and A. M. Echavarren, *J. Am. Chem. Soc.*, 2006, **128**, 5033–5040.

9 H. B. Kratz, M. E. van der Boom, Y. Ben-David and D. Milstein, *Isr. J. Chem.*, 2001, **41**, 163–171.

10 While the *N,N,N* pincer framework is anticipated to be inert, the possibility of a C_{aryl}–$N_{anilide}$ coupling reaction involving the anilide moiety of the *N,N,N* ligand represents an alternative pathway. For C_{sp3}–N coupling *via* high valent Pd, see for example: (*a*) S. R. Whitfield and M. S. Sanford, *J. Am. Chem. Soc.*, 2007, **129**, 15142–15143; (*b*) A. Iglesias and K. Muñiz, *Helv. Chim. Acta*, 2012, **95**, 2007–2025; (*c*) M. H. Perez-Temprano, J. M. Racowski, J. W. Kampf and M. S. Sanford, *J. Am. Chem. Soc.*, 2014, **136**, 4097–4100; (*d*) T.-S. Mai, X. Wang and J.-Q. Yu, *J. Am. Chem. Soc.*, 2009, **131**, 10806–10807; (*e*) P. A. Sibbald and F. E. Michael, *Org. Lett.*, 2009, **11**, 1147–1149; (*f*) P. A. Sibbald, C. F. Rosewall, R. D. Swartz and F. E. Michael, *J. Am. Chem. Soc.*, 2009, **131**, 15945–15951; (*g*) A. Iglesias, R. Alvarez, A. R. de Lera and K. Muiz, *Angew. Chem., Int. Ed.*, 2012, **51**, 2225–2228.

11 N. Sakai, K. Annaka and T. Konakahara, *J. Org. Chem.*, 2006, **71**, 3653–3655.

12 L. A. Wright, E. G. Hope, G. A. Solan, W. B. Cross and K. Singh, *Dalton Trans.*, 2015, DOI: 10.1039/c5dt00062a, Advance Article.

13 (*a*) M. Lopez-Torres, P. Juanatey, J. J. Fernandez, A. Fernandez, A. Suarez, D. Vazquez-Garcia and J. M. Vila, *Polyhedron*, 2002, **21**, 2063–2069; (*b*) H. Onoue and I. Moritani, *J. Organomet. Chem.*, 1972, **43**, 431–436; (*c*) H. Onoue, K. Minami and K. Nakagawa, *Bull. Chem. Soc. Jpn.*, 1970, **43**, 3480–3485.

14 O. Adeyi, W. B. Cross, G. Forrest, L. Godfrey, E. G. Hope, A. McLeod, A. Singh, K. Singh, G. A. Solan, Y. Wang and L. A. Wright, *Dalton Trans.*, 2013, **42**, 7710–7723.

15 W. B. Cross, E. G. Hope, G. Forrest, K. Singh and G. A. Solan, *Polyhedron*, 2013, **59**, 124–132.

16 K. Nakamoto, *IR and Raman Spectra of Inorganic and Coordination Compounds*, Wiley, New York, 5th edn, 1997, Part B, p. 271.

17 Characteristic HF signal in CD_3CN see: M. M. Shaw, R. G. Smith and C. A. Ramsden, *ARKIVOC*, 2011, 221–228.

18 W. L. F. Armarego and D. D. Perrin, *Purification of Laboratory Chemicals*, Butterworth Heinemann, 4th edn., 1996.

19 Y. D. M. Champouret, R. K. Chaggar, I. Dadhiwala, J. Fawcett and G. A. Solan, *Tetrahedron*, 2006, **62**, 79–89.

20 (*a*) P. Fitton and E. A. Rick, *J. Organomet. Chem.*, 1971, **28**, 287–291; (*b*) W. R. Moser, A. W. Wang and N. K. Kildahl, *J. Am. Chem. Soc.*, 1988, **110**, 2816–2820.

21 G. M. Sheldrick, *SHELXTL Version 6.10*, Bruker AXS, Inc. Madison, Wisconsin, USA, 2000.